BBA - Molecular Basis of Disease 1865 (2019) 165520

Contents lists available at ScienceDirect

BBA - Molecular Basis of Disease

journal homepage: www.elsevier.com/locate/bbadis

Elimination of KLK5 inhibits early skin tumorigenesis by reducing epidermal proteolysis and reinforcing epidermal microstructure

Georgios Pampalakis[a], Eleni Zingkou[a], Lucas Kaklamanis[b], Magda Spella[c], Georgios T. Stathopoulos[c], Georgia Sotiropoulou[a,*]

[a] Department of Pharmacy, School of Health Sciences, University of Patras, 265 04 Rio, Greece
[b] Department of Pathology, Onassis Cardiac Surgery Center, Athens, Greece
[c] Laboratory for Molecular Respiratory Carcinogenesis, Department of Physiology, Faculty of Medicine, University of Patras, 26504 Rio, Greece

ARTICLE INFO

Keywords:
Kallikrein-related peptidase 5 (Klk5)
Proteolysis
Desmosomes
Desmoglein 1
Inflammation
Skin cancer

ABSTRACT

Epidermal desquamation involves a finely-tuned proteolytic cascade ensuring the regulated cleavage of desmosomes that releases old stratum corneum outermost layers. Although the roles of desmosomes in normal physiology are well-established, their putative involvement in cancer remains unexplored. The KLK5 protease is thought of having fundamental roles in epidermal proteolysis and homeostasis, and its aberrant activity has been linked to skin pathologies. We found that deletion of Klk5 results in significantly higher numbers of lengthier desmosomes and enhanced skin strength. *Klk5*$^{-/-}$ mice retained normal skin barrier function and are resistant to chemically-induced skin tumorigenesis. The resistance to tumorigenesis was not due to inhibition of inflammation, and on the contrary, absence of *Klk5* increased the TPA-induced inflammatory skin response. We found that increased desmosomes and reduced proteolysis prevent oncogenic signaling by capturing β-catenin into the cytoplasm and facilitate epidermal keratinocyte apoptosis, thus, inhibiting tumor initiation. We highlight that the skin ultrastructure affects early neoplastic transformation by modulating intracellular signaling and suggest that tissue reinforcement provides a novel mode of tumor suppression.

1. Introduction

Desmosomes constitute intercellular adhesive junctions that are present on the lateral side of neighboring polarized epithelial cells. Originally visualized as static protein complexes that fortify cell adhesion against shearing forces and physical stress and increase mechanical strength, it is now understood that desmosomes can also modify intracellular signals to regulate cell proliferation and differentiation [1,2]. The crucial role of desmosomes in physiology is highlighted in the epidermis, where deficiency in their protein components results in severe, often lethal disorders [3]. In particular, the key role of desmoglein 1 (DSG1) in maintaining epidermal integrity is demonstrated in *pemphigus foliaceus*, an autoimmune disease where presence of anti-DSG1 antibodies in patients' sera cause superficial skin blistering [4]. DSG1 is also the substrate of the exfoliative toxin A, a serine protease produced by *Staphylococcus aureus*, the causative factor of staphylococcal scalded-skin syndrome [5]. Recently, *DSG1* deficiency was linked to severe dermatitis, multiple allergies and metabolic wasting (SAM) syndrome [6].

Desmosomes regulate cell proliferation and differentiation by affecting Wnt/β-catenin signaling [1,2]. Loss or dysfunction of desmosomes facilitates the release of plakoglobin (JUP) leading to nuclear translocation of β-catenin and activation of β-catenin signaling [1]. Since desmosomes regulate the strength of cell-cell adhesion, they could be implicated in cancer development and/or progression but their specific role(s) remain largely elusive. Previous studies have shown that epidermal deletion of *Perp*, encoding a protein that promotes the assembly and stabilization of desmosomes, results in loss of desmosomes, which promotes initiation and progression of UVB-induced squamous cell carcinomas by enhancing cell survival and skin inflammation, while inhibiting apoptosis [7]. Additionally, the inducible conditional ablation of *Perp* in epidermis confers resistance to DMBA/TPA-induced skin papillomas (Marques et la., 2005). However, conditional deletion of *Perp* mediated by K5-Cre results in 40% lethality of the generated mice (Marques et la., 2005), while inducible deletion with K14-CreER results in occasional blistering in mice ([8]b), posing questions whether their epidermal barrier is normal. In general, studies on whether and how desmosomes may be linked to cancer development or/and progression were hindered by the fact that mouse models deficient in any of the desmosomal proteins suffer perinatal lethality [1].

* Corresponding author at: Department of Pharmacy, School of Health Sciences, University of Patras, Rion-Patras 265 04, Greece.
E-mail address: gdsotiro@upatras.gr (G. Sotiropoulou).

https://doi.org/10.1016/j.bbadis.2019.07.014
Received 20 March 2019; Received in revised form 13 July 2019; Accepted 27 July 2019
Available online 02 August 2019

Physiological skin desquamation depends on the tightly regulated cleavage of desmosomal structures in the stratum corneum by KLK proteases [9,10]. The corneodesmosomal components DSG1, desmocollin 1 (DSC1) and corneodesmosin (CDSN) are specific *in vivo* substrates recognized by KLK5 for proteolytic cleavage [11,12]. KLK5 is considered the upstream activator of the epidermal proteolytic cascade, since it is able to autoactivate and, subsequently, mature KLK5 activates other downstream KLK and non-KLK zymogens thus, augmenting the proteolytic activities in epidermis [13–15]. With the aim to validate the role of KLK5 as a key regulator of epidermal proteolysis, we generated *Klk5*$^{-/-}$ mice and found that their epidermis exhibits significantly elevated levels of Dsg1 and highly increased number of desmosomes. This finding prompted us to exploit *Klk5*$^{-/-}$ mice as a model to investigate the role of desmosomes in skin cancer. We found that elimination of Klk5 remarkably suppresses the number of chemically induced skin tumors. We propose that increased number of desmosomes in *Klk5*$^{-/-}$ skin is associated with cytoplasmic localization of β-catenin, which confers resistance to tumor growth in *Klk5*$^{-/-}$ skin. These findings provide compelling *in vivo* evidence for the crucially protective role of skin microstructures against cancer.

2. Material and methods

2.1. Ethics statement

All animal work has been done in accordance with protocols approved by the Bioethics Committee of the University of Patras in accordance with the European Legislation. All human samples were obtained under the permission of the patients and in accordance with the ethical standards of the Helsinki Declaration.

2.2. Materials

Chemicals were obtained from Sigma or Merck. Anti-KLK5 antibody was a gift from Prof. Eleftherios Diamandis. Antibody against β-catenin was from Abgent (AJ1092a), against desmoglein 1 from Santa Cruz (sc-20114), against α-tubulin from Sigma (T5168) and for cleaved caspase 3 from Cell signaling (9661). All primers were obtained from Invitrogen and are shown in Supplementary Table 1. Genomic DNAs were extracted with GenElute mammalian DNA extraction (Sigma) and total RNAs with Nucleospin RNA (Macherey-Nagel).

2.3. Generation of Tg-NglKlk5$^{-/-}$ mice

Klk5$^{-/-}$ on C57BL/6 background were intercrossed with *Ngl* transgenic mice [16], also on C57BL/6 background, to generate the Tg-*NglKlk5*$^{+/-}$. Then, the Tg-*NglKlk5*$^{+/-}$ were intercrossed with *Klk5*$^{-/-}$ to generate Tg-*NglKlk5*$^{-/-}$. For monitoring Nf-κb activity *in vivo*, mice were anaesthetized with isoflurane and 1 mg luciferin in 100 μl of PBS was injected in the retroorbital venous. Luciferase activity was monitored with the IVIS bioluminescence imaging under anesthesia.

2.4. RT-PCR

Total RNAs from mice tissues were extracted, reverse transcribed with Superscript II (Invitrogen) and the resulting cDNAs were amplified by PCR using gene-specific primers (Table S2). Alternatively, total RNA was used as template for one-step RT-qPCR (Kapa SYBR Fast).

2.5. Electron microscopy

For scanning electron microscopy (SEM), skin tissue samples were surgically removed, fixed in 4% formaldehyde in PBS for 24 h, washed and dehydrated in a series of ethanol baths. Ethanol was replaced with acetone, samples were dried, gold sputtered and observed in field emission SEM. For transmission electron microscopy (TEM), skin samples from newborn mice were fixed in 2% glutaraldehyde, 4% paraformaldehyde in 0.1 M cacodylate buffer pH 7.2 for 24 h, then, washed, and stained in 1% OsO_4 in cacodylate for 2 h at room temperature. Finally, they were dehydrated in a series of acetone baths and embedded in epoxy-resin (Sigma). Blocks were cut in thin sections (50 μm), placed on grids, stained with $UO_2(CH_3COO)_2$ and lead citrate and observed under TEM (Challenger, 40 kV).

2.6. Western blotting and gel zymography

Tissues were pulverized under liquid N_2 with a pestle and mortar, and proteins were extracted in lysis buffer (50 mM Tris-HCl, pH 7.5, 150 mM NaCl, 1% Triton X-100) for 30 min at 4 °C. Protein concentrations were determined by Bradford assay (Biorad). For Western blotting, protein extracts were run on SDS-PAGE, electroblotted on PVDF membrane and probed with the appropriate antibodies. For gel zymography, extracts were resolved on 12% SDS-PAGE containing 0.1% gelatin. Gels were washed twice with 50 mM Tris-HCl pH 7.5, 5 mM $CaCl_2$, 2.5% Triton X-100 for 15 min, 15 min with 50 mM Tris-HCl, pH 7.5, 5 mM $CaCl_2$, 0.1% Triton X-100, then, incubated in the latter buffer for 24 h and finally stained with Coomassie G-250.

2.7. Chemical carcinogenesis

Skin tumors were induced chemically by application of DMBA/TPA or DMBA/DMBA. Three days prior to chemical application, 7–9 weeks old mice were depilated with Veet cream. Each animal received 50 μg of DMBA in 100 μl of acetone bilaterally on each flank. After 2 days mice received 100 μl of $2*10^{-4}$ M TPA in each flank twice-weekly for the DMBA/TPA protocol or 10 μg of DMBA in 100 μl acetone for the DMBA/DMBA protocol for a total of 15 weeks. Mice were visually inspected for the appearance of papillomas twice a week. Tissues were collected in OCT (Optimal Cutting Temperature, Sakura) for histological analysis.

2.8. Irritant contact dermatitis (ICD or ear swelling test)

ICD was induced by applying 40 nmoles of TPA in 20 μl of acetone on the right ear of 8 week old anaesthetized mice. After 24 h, ears were harvested, weighted, and their thickness was measured. Tissues were homogenized under liquid N_2, weighted, resuspended in 100 μl distilled H_2O, lysed by 3× repeated freeze-thawing (−70 °C to 37 °C) and the haemoglobin content was determined by Drabkin reagent and expressed as absorbance at 540 nm normalized against the tissue weight.

2.9. Histology and TUNEL assay

Tissues were excised, cut and stored in OCT. Samples were cut in 5 or 10 μm sections. Sections were fixed for 5 min in acetone and stained with eosin/haematoxylin. Alternatively, tissues were fixed for 24 h in 4% formaldehyde in PBS, embedded in paraffin, and processed as described [17]. For immunohistochemistry (IHC), and immunofluorescence (IF), cryosections were processed as previously [17]. Terminal deoxynucleotidyl transferase-mediated dUTP nick end labeling was conducted with the *in situ* cell death detection reagent (Roche). Apoptotic cells were quantified as the number of positive cells relative to the total number of epidermal cells per optical field and expressed as % of positive cells. Two sections per mouse (n = 3 mice per genotype) were stained and used for TUNEL quantification. All microscope images were taken on Zeiss optical microscopes with the aid of Axion Vision software (Zeiss) and analyzed by either the same program or with ImageJ.

2.10. In situ zymography

Skin cryosections (5 μm) were mounted on glass slides, rinsed with 2% Tween 20 in PBS and incubated for 3 h at 37 °C with 100 μg ml^{-1}

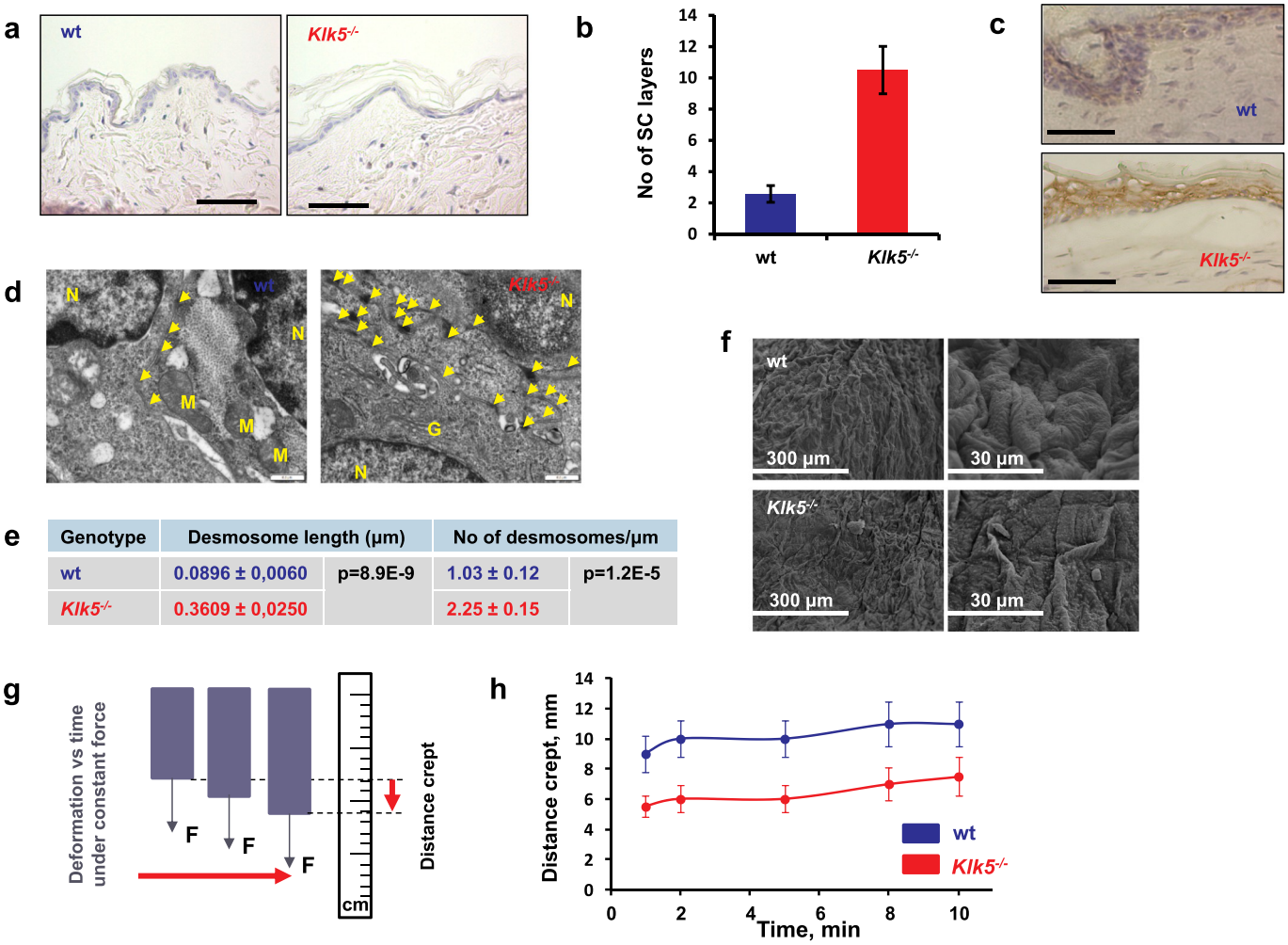

Genotype	Desmosome length (μm)		No of desmosomes/μm	
wt	0.0896 ± 0,0060	p=8.9E-9	1.03 ± 0.12	p=1.2E-5
Klk5$^{-/-}$	0.3609 ± 0,0250		2.25 ± 0.15	

Fig. 1. Microscopic and macroscopic observation of *Klk5*$^{-/-}$ mice. **a** Haematoxylin and eosin (H&E) staining of paraffin embedded skin tissue sections from wt and *Klk5*$^{-/-}$ mice (6 months age) shows hyperkeratosis in *Klk5*$^{-/-}$ epidermis. Scale bar: 20 μm. **b** Quantification of stratum corneum layers from a (n = 3). **c** IHC staining of frozen skin sections for Dsg1 shows strong expression in the epidermis of newborn *Klk5*$^{-/-}$ mice. Scale bar: 20 μm. **d** Transmission electron microscopy images show markedly increased number of desmosomes (indicated with yellow arrows) in *Klk5*$^{-/-}$ epidermis; N, nucleus; M, mitochondrion; G, Golgi. Scale bar: 0.5 μm and 0.2 μm for the smaller image on the right. **e** Quantification of desmosome density and length. Data were obtained by measuring 80 desmosomes per genotype and shown as mean ± SD. **f** Scanning electron microscopy images of *Klk5*$^{-/-}$ and wt epidermis show that *Klk5*$^{-/-}$ epidermis is wrinkled. **g** Schematic diagram of the tissue creep assay. **h** Measurements of tissue creep were obtained at the indicated time points under constant tension. Data represent mean ± SE (n = 3 and 4 for wt and *Klk5*$^{-/-}$ animals, respectively).

BODIPY FL casein (Life Technologies) in 50 mM Tris-HCl, pH 8.0. Sections were rinsed with PBS, mounted with mowiol and visualized with a Leica TCS SP5 confocal laser-scanning microscope (CLSM). Data were analyzed using ImageJ.

2.11. Skin creep assay

Skins from the flank of 8 week old male mice were cut in 2 cm × 3 cm pieces and from one side they were stably attached on a vertical stage and on the other side, a constant weight of 42 g (0.412 Newtons) was attached. A fixed scale was used to determine the length of the skin. The deformation (length) of skin *versus* time was recorded for a period of 10 min.

2.12. In silico gene expression

The data on *Klk5* expression in the DMBA/TPA mouse skin carcinogenesis model were obtained from Gene Expression Omnibus (accession number: GSE21264) and analyzed with GEO2R. This dataset was obtained in Alain Balmain's group [18] using Affymetrix Mouse Genome 430 2.0 arrays and encompasses normal skin from mice tails (n = 80), papillomas (n = 60) and carcinomas (n = 68). IHC data for KLK5 expression were retrieved from the Human Protein Atlas (http://www.proteinatlas.org).

2.13. Analysis of human samples

10 normal skin, 10 hyperplastic lesions, 12 keratoacanthomas, 6 non-invasive *in situ* squamous carcinomas and 15 invasive squamous carcinomas of various differentiation patterns were IHC stained for KLK5 expression.

2.14. Par2 activation

Par2 activity was determined in epidermal extracts based on the cleavage of the quenched synthetic peptide (Abz-Ser-Lys-Gly-Arg-Ser-Leuc-Ile-Gly-Lys(Dnp)-Asp-OH), a Par2 specific substrate. Briefly, 6.4 μM Abz-Ser-Lys-Gly-Arg-Ser-Leu-Ile-Gly-Lys(Dnp)-Asp-OH in 0.1 M HEPES, 0.1 M NaCl, 10 mM $CaCl_2$, 0.2% polyethelene glycol, pH 7.4 were equilibrated at 37 °C for 10 min and, then, 50 μg of total epidermal protein extracts were added and activity was determined by monitoring the fluorescence (λ_{ex} = 325 nm, λ_{em} = 414 nm) for 3 min.

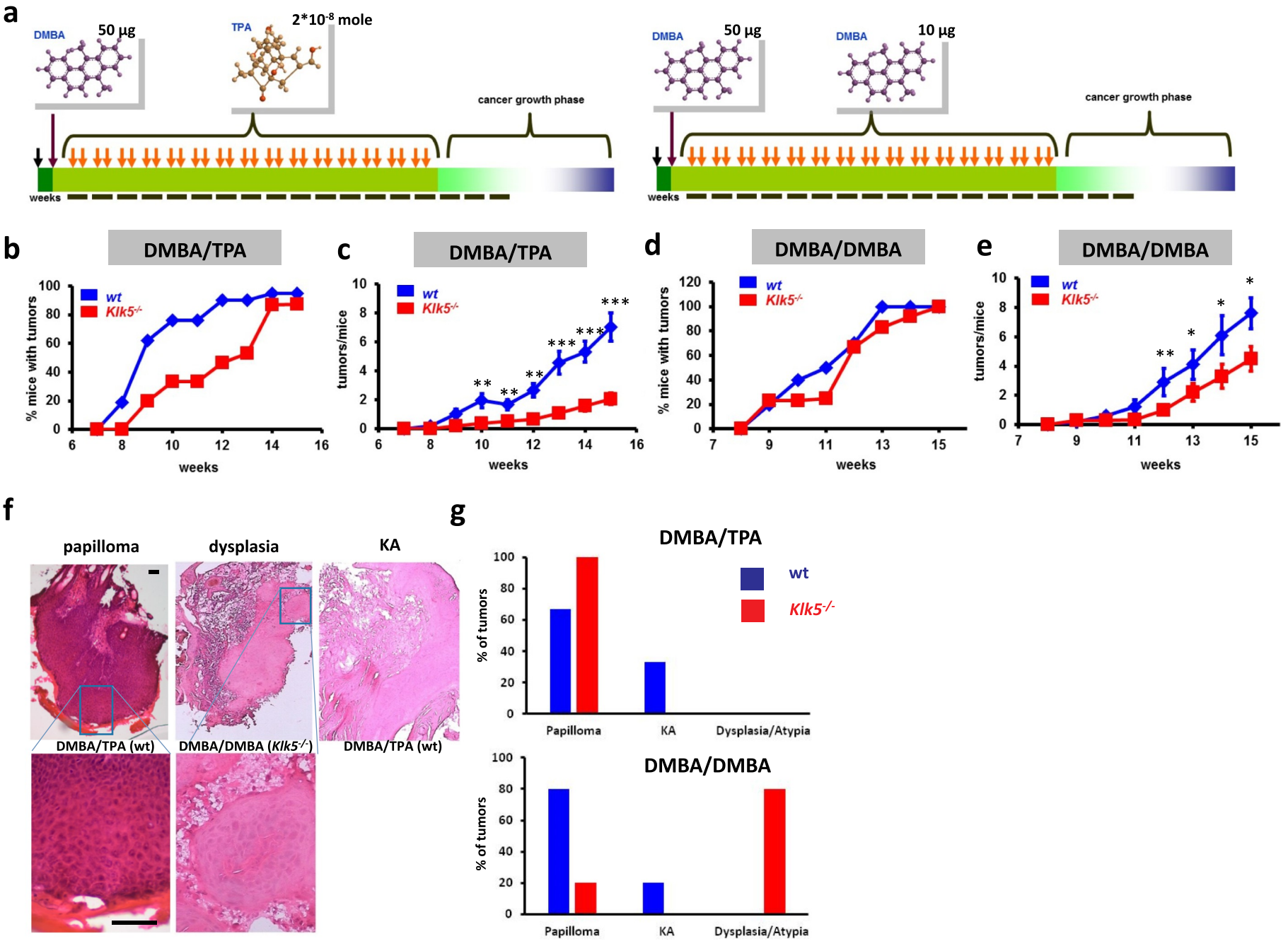

(caption on next page)

Fig. 2. Deletion of *Klk5* suppresses the development of skin tumors. **a** The schemes applied for chemical carcinogenesis are shown. DMBA-initiated and TPA-promoted (DMBA/TPA) is shown on the left and DMBA-initiated and DMBA-promoted (DMBA/DMBA) on the right. **b** % of mice with tumors growth in wt *vs* $Klk5^{-/-}$ mice following DMBA/TPA. **c** time course of papilloma growth (number of tumors) in wt *vs* $Klk5^{-/-}$ mice following DMBA/TPA. **d** % of mice with tumors growth in wt *vs* $Klk5^{-/-}$ mice following DMBA/DMBA. **e** time course of papilloma growth (number of tumors) in wt *vs* $Klk5^{-/-}$ mice following DMBA/DMBA. The DMBA/TPA group included 21 wt and 15 $Klk5^{-/-}$ and the DMBA/DMBA group 10 wt and 13 $Klk5^{-/-}$ mice. Data represent mean ± SD. *p < 0.05, **p < 0.005, ***p < 0.0005. **f** Representative images of papilloma, keratoacanthoma, and dysplasia developed in mice. Scale bars: 50 μm. **g** distribution of tumors developed in DMBA/TPA model (n = 9 and 5 for wt and $Klk5^{-/-}$) and in DMBA/DMBA model (n = 5 and 5 for wt and $Klk5^{-/-}$).

2.15. Wound healing

8–10 weeks old male mice were depilated and animals at the telogen phase (pink color) were selected. Three days later, wounds were induced with 4 mm punch biopsies. The wounds were photographed and the area was quantified with the ImageJ and expressed as percentage of wound remaining open *vs* time.

2.16. Epidermal turnover

8–10 weeks old male mice were depilated 3 days prior to the experiment. Subsequently, 5% (wt/vol) dansyl chloride in Nivea body milk was applied onto the mouse back [19]. Samples of back skin were excised under anesthesia after 4 and 48 h and stored in OCT. 20 μm cryosections were fixed in acetone, mounted with mowiol and observed under a fluorescence microscope (Nikon TE2000U) with DAPI filter.

2.17. Statistics

The data presented as mean values ± standard deviation (S.D.) or standard error (S.E.) as indicated. Statistical significance was determined with Student's *t*-test. The number of mice used in the experiments is indicated in the relative sections.

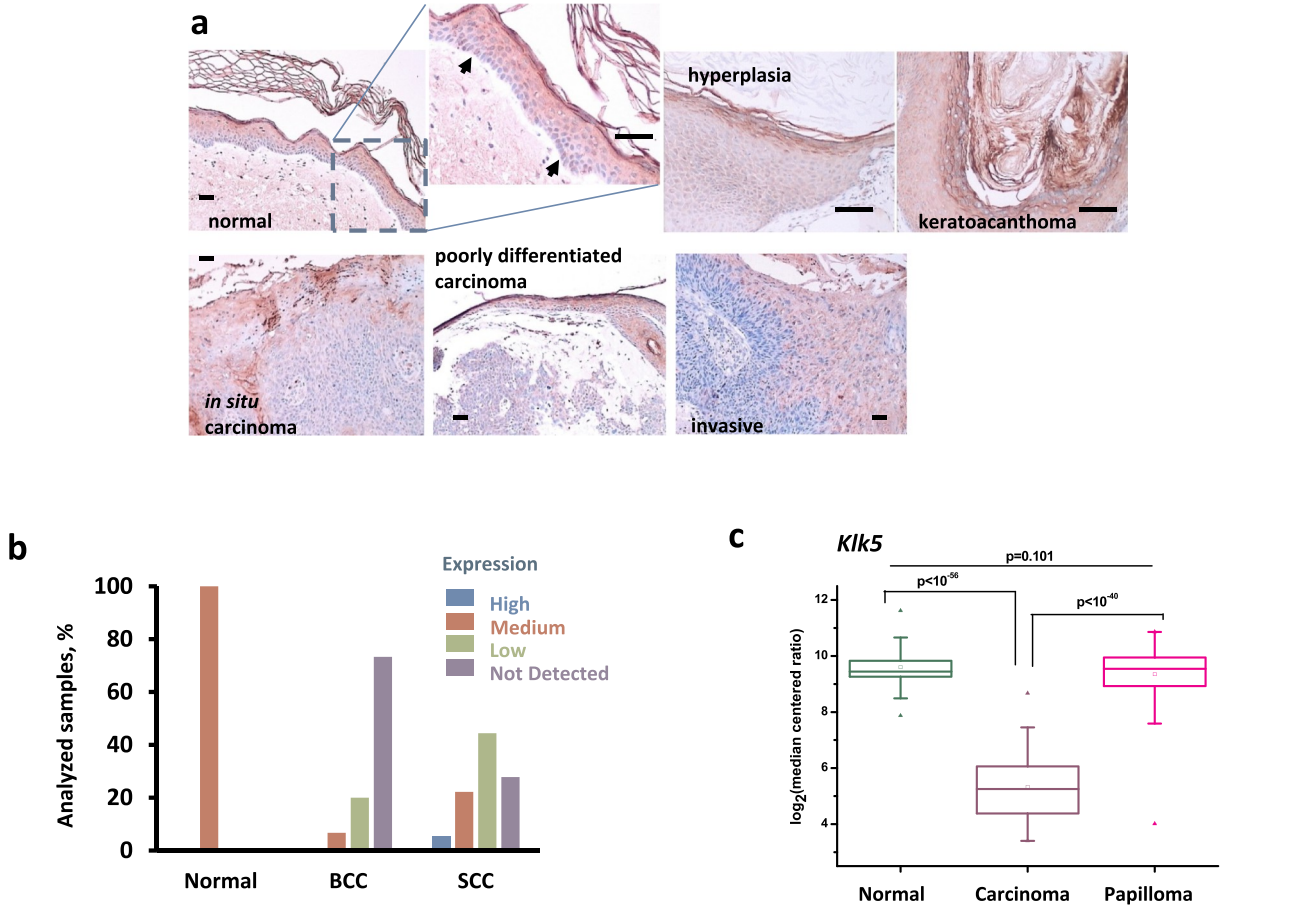

Fig. 3. a In normal human epidermis KLK5 is expressed and found in the cytoplasm. Strong staining can be seen in the stratum corneum. In the basal cell layer nuclear membranous staining is also identified (marked by arrows). KLK5 shows similar expression pattern in hyperplasias and keratoacanthomas. In *in situ* carcinoma gradual loss of KLK5 expression is observed. Loss of KLK5 expression is also seen in poorly differentiated carcinomas (On the top, normal expression can be seen). In invasive carcinomas there is maintenance of KLK5 expression in the more differentiated areas of the tumor and loss of KLK5 expression with loss of squamoid differentiation (10 normal skin, 10 hyperplastic lesions, 12 keratoacanthomas, 6 non-invasive *in situ* squamous carcinomas and 15 invasive squamous carcinomas of various differentiation patterns). Scale bars: 50 μm. **b** Results of IHC analysis of KLK5 expression with the protein atlas (n = 6 normal, n = 15 basal cell carcinoma, n = 18 squamous cell carcinoma). KLK5 expression is greatly reduced or absent in basal and squamous cell carcinoma samples compared to normal skin. **c** Comparative bioinformatic analysis of the Balmain's microarray dataset (GSE21264) for mouse normal skin, papillomas and carcinomas (induced by DMBA/TPA treatment) demonstrates that the expression of *Klk5* is reduced in carcinomas.

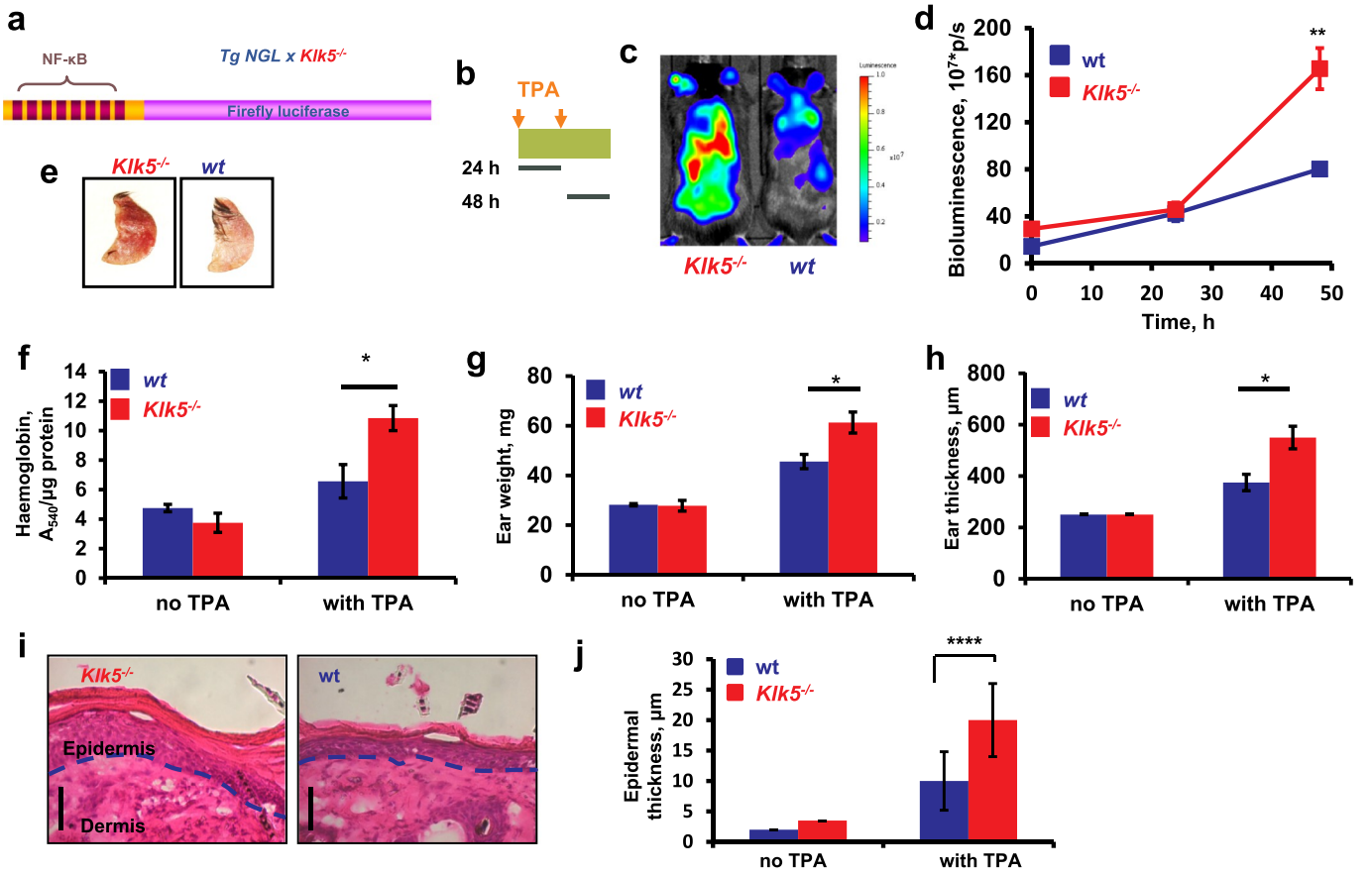

Fig. 4. Absence of Klk5 is associated with enhanced skin Nf-κb activation and inflammation. **a** Schematic representation of the reporter luciferase gene integrated in Tg-*Ngl* mice. Nf-κb reporter is under the control of a minimal promoter carrying eight Nf-κb consensus sequences upstream of the firefly luciferase gene. **b** Schematic representation of the TPA application protocol for induction of skin inflammation. Each dose of TPA was 20 nmoles. **c** and **d** Nf-kb activity is strongly induced by TPA in *Klk5*$^{-/-}$ skin. Representative mice from each genotype are shown after two applications of TPA. Quantified data are shown as mean ± SE (n = 10 and 8 for wt and *Klk5*$^{-/-}$, respectively). **e** The ears of *Klk5*$^{-/-}$ mice appear erythematous after TPA application. **f** *Klk5*$^{-/-}$ ears contain significantly higher amounts of haemoglobin compared to wt, which is consistent with the observed erythema and bleeding. Ear weight **g** and thickness **h** were both significantly increased in *Klk5*$^{-/-}$ indicating extensive edema. **i** H&E stained cryosections of skin tissue isolated from mice treated twice with TPA demonstrate huge acanthosis in *Klk5*$^{-/-}$ epidermis. Scale bar: 20 μm. **j** Quantification of epidermal thickness (n = 4 and 5 for wt and *Klk5*$^{-/-}$, respectively). Data represent mean ± SE *p < 0.05, **p < 0.005, ****p < 1E-5.

3. Results

3.1. Characterization of *Klk5*$^{-/-}$ mice

The generation of *Klk5*$^{-/-}$ mice has been described previously [20]. *Klk5*$^{-/-}$ mice are macroscopically indistinguishable from the wt and fertile. Histological examination showed hyperkeratosis without other apparent skin abnormalities (Fig. 1A-B). The levels of Dsg1 are significantly increased (Fig. 1C) providing *in vivo* evidence that Dsg1 could be a substrate of the Klk5 protease. Consistently, TEM of the epidermis ultrastructure revealed that desmosomes are significantly increased in number, length and electron density in *Klk5*$^{-/-}$ compared to wt mice, as clearly shown in Fig. 1D–E. SEM showed that the surface of *Klk5*$^{-/-}$ mice appears rather wrinkled probably due to hyperkeratosis (Fig. 1F). Previously we have shown that the functionality of the epidermal barrier, remains intact [20]. No compensatory effects have been found in *Klk5*$^{-/-}$, namely severe alterations in the expression of other *Klk* genes [21]. Finally, decreased skin creep in *Klk5*$^{-/-}$ mice was found (Fig. 1G–H), pointing to tissue reinforcement and enhanced mechanical linkage caused by the increased number of desmosomes.

3.2. *Klk5*$^{-/-}$ mice are resistant to skin carcinogenesis

We subjected *Klk5*$^{-/-}$ and wt mice to two different schemes of chemically induced skin carcinogenesis, as depicted in Fig. 2A. In the DMBA/TPA scheme there was a delay in the tumor onset (Fig. 2B–C). There were no significant alterations in the percentage of mice with tumors. However, the number of tumors induced by DMBA/TPA was largely suppressed in *Klk5*$^{-/-}$ and to a lesser extent in the DMBA/DMBA model (Fig. 2D–E). We histologically assessed different tumors obtained after 22 weeks in order to examine their progression. All DMBA/TPA tumors derived from wt animals were either papillomas or keratoacanthomas, while tumors developed in *Klk5*$^{-/-}$ animals were papillomas (Fig. 2F–G). Probably due to the very low total number of tumors grew in *Klk5*$^{-/-}$ it was very difficult to find tumors that have progressed to other stages. Therefore, we also studied the tumors developed by DMBA/DMBA methodology that in contrast to DMBA/TPA, can result in *de novo* formation of papillomas and carcinomas. We found that in wt mice, tumors were mainly papillomas while in *Klk5*$^{-/-}$ most of the tumors examined had developed dysplasias or atypias (Fig. 2G).

3.3. Expression of KLK5 in human skin cancer specimens

We analyzed a series of clinical specimens for the expression of KLK5 with IHC to address its role in human carcinogenesis. As shown in Fig. 3A, we found that KLK5 is expressed in normal epidermis, while hyperplastic lesions (papillomas) and keratoacanthomas display similar expression to normal. In more advanced stages of cancer KLK5

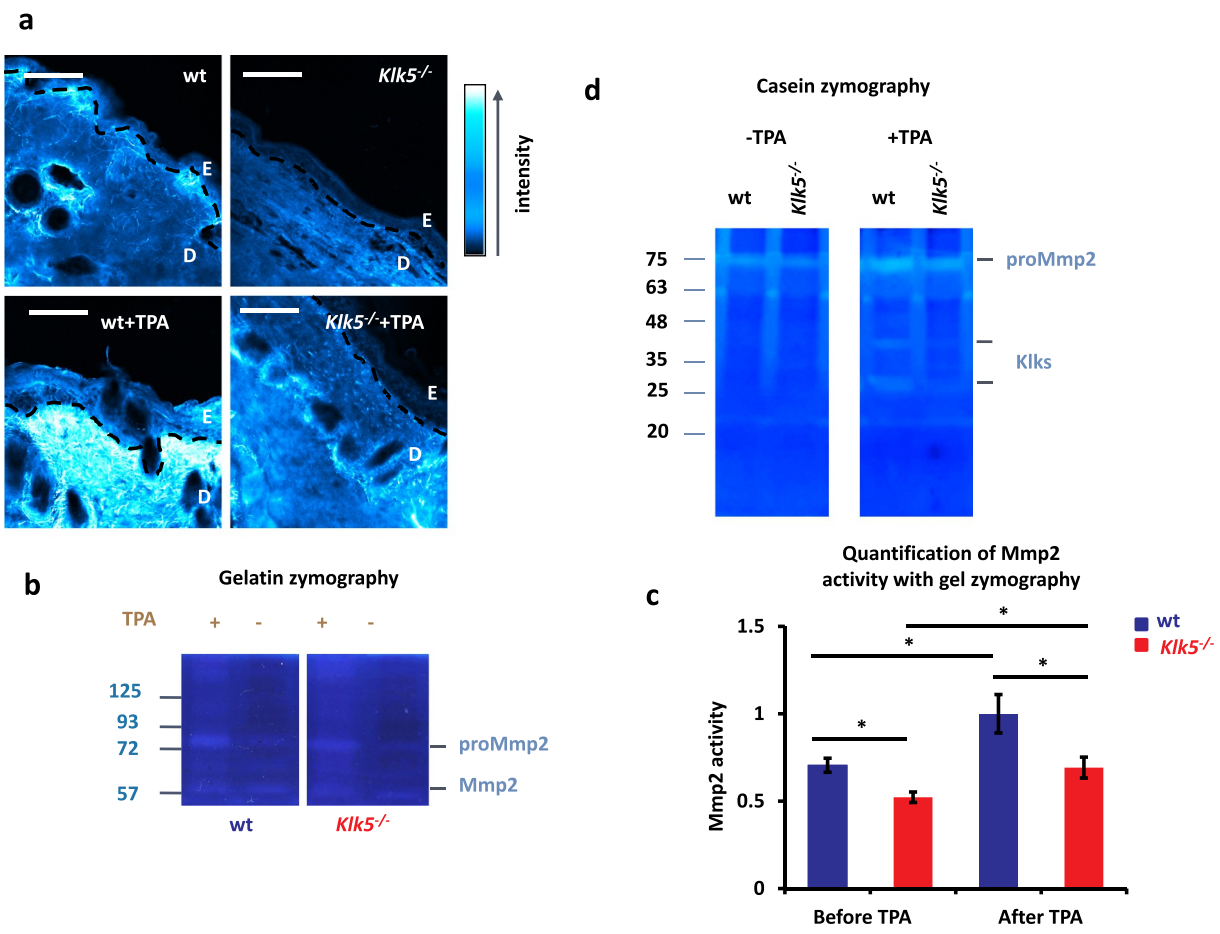

Fig. 5. Differential response of *Klk5*$^{-/-}$ and wt epidermis to TPA. **a** *In situ* zymography with casein substrate. Elimination of Klk5 results in slightly lower epidermal and dermal proteolysis but in remarkable suppression of overall proteolysis after TPA application compared to wt skin. The dashed line indicates the epidermis-dermis junction. Scale bars: 20 μm. E, epidermis; D, dermis. **b** Representative gelatin zymography of extracts prepared from TPA treated and untreated wt and *Klk5*$^{-/-}$ skin. In total three animals per genotype were analyzed. ProMmp2 and active Mmp2 are both increased by TPA and to a higher extent in *Klk5*$^{-/-}$ skin compared to wt. Sizes on the left are given in kilodaltons (kDa). **c** Quantification of Mmp2 activity by gelatin zymography after TPA application (n = 3 per genotype, *p < 0.01). **d** Representative casein zymography of extracts prepared from TPA treated and untreated wt and *Klk5*$^{-/-}$ skin. The bands between 25 and 40 kDa are consistent with members of the Klk family, likely Klk7 and Klk5.

expression is lost. IHC data retrieved from human protein atlas confirmed our analysis showing lower expression in squamous cell carcinomas (SCC) and basal cell carcinomas (BCC) compared to normal (Fig. 3B). Analysis of publicly available microarray data from DMBA/TPA-induced papillomas and carcinomas [18] showed that *Klk5* expression is reduced in carcinomas (Fig. 3C). Taken together these results indicate that reduced KLK5 expression is associated with progression of early-stage skin tumors to malignancy both in human and mice, but whether and how it is functionally involved merits further investigation.

3.4. Augmented Nf-κb activity and inflammation in *Klk5*$^{-/-}$ skin

Due to the involvement of KLK5 hyperactivity in epidermal Nf-κb activation and subsequent induction of skin inflammation in Netherton syndrome (NS) [17] and cancer [22], we hypothesized that absence of Klk5 could inhibit the inflammatory reaction during the promotion phase of chemical carcinogenesis, thus inhibiting the formation of tumors. To test the activation of Nf-κb in *Klk5*$^{-/-}$ skin, we have crossed *Klk5*$^{-/-}$ mice with transgenic *Ngl* that carry an Nf-kb responsive promoter upstream of the firefly luciferase gene (Fig. 4A) to generate Tg-*Ngl/Klk5*$^{-/-}$ mice. Tg-*Ngl/Klk5*$^{-/-}$ were epicutaneously challenged with TPA (Fig. 4B) and surprisingly strong Nf-kb activity in *Klk5*$^{-/-}$ epidermis was detected (Fig. 4C–D).

Then, we induced inflammation by applying TPA onto the mouse ear. Contrary to wt, *Klk5*$^{-/-}$ mice developed marked edema and redness (Fig. 4E) indicative of hyperaemia accompanied by extensive bleeding following ear dissection (Fig. 4F) and increased haemoglobin content (Fig. 4H). The extent of edema was quantified based on the thickness and weight of the ear, which both were significantly increased in *Klk5*$^{-/-}$ animals (Fig. 4G–H). Cutaneous TPA application on mouse back, resulted in a more pronounced epidermal thickening of *Klk5*$^{-/-}$ (Fig. 4I–J) in direct relation to the results obtained with the ear swelling assay. In summary, chemically induced inflammatory response is exaggerated in the absence of *Klk5*.

3.5. Suppressed proteolysis in *Klk5*$^{-/-}$ epidermis inhibits β-catenin activation and induces apoptosis in inflamed skin

Since Klk5 is considered a major regulator of skin proteolysis based on *in vitro* studies [14,15], the overall proteolytic activities were determined before and after TPA application. *In situ* and gel zymography showed that prior to TPA application the overall proteolytic activities in *Klk5*$^{-/-}$ epidermis were slightly lower than in wt. TPA induces epidermal proteolysis in both wt and *Klk5*$^{-/-}$, however in *Klk5*$^{-/-}$ the induction of proteolysis (in particular Mmp2 and Klks) was significantly lower than in wt (Fig. 5).

TPA highly induces the expression of *Klk5* (Fig. 6A) that could

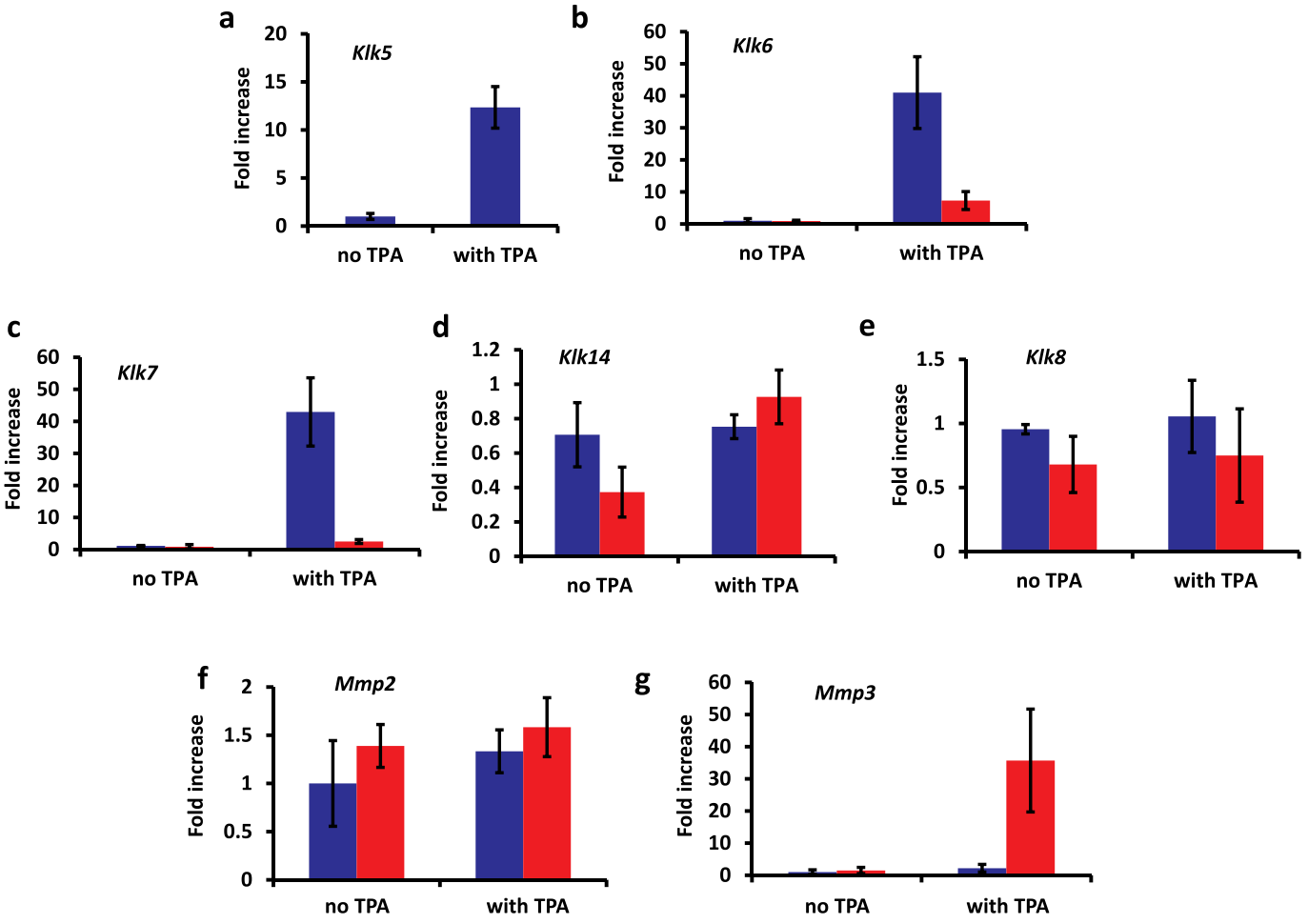

Fig. 6. Reduced expression of Klks in *Klk5*$^{-/-}$ epidermis after TPA application. **a** TPA induces the expression of *Klk5* mRNA in wt skin, implicating a potential role of Klk5 during tumor promotion. **b–c** Expression of *Klk6* and *Klk7* mRNAs display significantly stronger response in wt than in *Klk5*$^{-/-}$ skin. **d–e** Expression of *Klk14* and *Klk8* mRNAs is not significantly altered by TPA application. **f** Expression of *Mmp2* mRNA is not significantly altered by TPA application. **g** Expression of *Mmp3* mRNA is highly induced in the *Klk5*$^{-/-}$ epidermis by TPA. Real-time RT-PCR data are shown as mean ± SE (n = 3 and 4 for wt and *Klk5*$^{-/-}$, respectively). Red bars indicate expression in *Klk5*$^{-/-}$ skin and blue in wt skin. *Hprt* was used as normalization control for fold-increase measurements.

explain the highly elevated overall proteolysis displayed by wt, in concert with the remarkably induced expression of *Klk6* and *Klk7* (Fig. 6B–C) but not *Klk8* and *Klk14*, which are also expressed in epidermis (Fig. 6D–E). Further, *Mmp2* mRNA levels are not altered by TPA in *Klk5*$^{-/-}$ or wt epidermis (Fig. 6F). Taken together, Figs. 5 and 6 demonstrate that the reduced activity of Klks is due to reduced mRNA expression, which is not true for Mmp2. Fig. 6G shows surprisingly elevated *Mmp3* levels in TPA-treated *Klk5*$^{-/-}$ epidermis. Mmp3 is a well-characterized tumor suppressing protease that prevents tumor initiation in chemical carcinogenesis [38].

Reduced proteolysis in TPA-treated *Klk5*$^{-/-}$ epidermis is consistent with higher levels of Dsg1 (Fig. 7A). On the other hand, Par2 signaling activates β-catenin [23], a known promoter of non-melanoma skin cancer [24]. Since reduced KLK proteolysis could suppress Par2 we hypothesized that suppression of proteolysis could also influence the subcellular localization of β-catenin. Upon TPA promotion, β-catenin is translocated into the nucleus in wt epidermis but remains cytoplasmic in *Klk5*$^{-/-}$ (Fig. 7B–C). Nevertheless, we did not find increased Par2 activation after TPA application in *Klk5*$^{-/-}$ and wt epidermis (Fig. 7D) indicating that suppression of β-catenin activation in *Klk5*$^{-/-}$ is not related to inhibition of Par2 signaling. Another reason that accounts for holding β-catenin in the cytoplasm is the higher number of desmosomes in the *Klk5*$^{-/-}$ epidermis.

Inhibited β-catenin signaling induces apoptosis in esophageal carcinoma cells through Casp3 activation, suggesting a role of β-catenin in the regulation of apoptosis [37]. On the other hand, loss of desmosomal components such as Dsg1 leads to increased cell survival and resistance to apoptosis [1], and shRNA-mediated reduction of Dsg1 expression protects UV-induced apoptosis in keratinocytes [36]. Figs. 7E–F show remarkably elevated numbers of apoptotic keratinocytes in the epidermis of *Klk5*$^{-/-}$ mice following TPA application and consistently increased staining for cleaved caspase 3 (Fig. 7G). Cumulatively, we show that reduced epidermal proteolysis during TPA application results in inhibition of oncogenic β-catenin signaling and increased Dsg1 levels in *Klk5*$^{-/-}$ epidermis both associated with an elevated apoptotic response, which explain why tumorigenesis is suppressed in *Klk5*$^{-/-}$ skin.

3.6. Accelerated turnover in *Klk5*$^{-/-}$ epidermis

Reduced tumor incidence associates with rapid epidermal turnover that accounts for the loss of DMBA-mutated keratinocyte stem cells that are considered the source of chemically induced tumors [19]. To test this, we fluorescently labeled the stratum corneum with dansyl chloride and quantified the remaining fluorescence after 2 days. As shown in Fig. 8A–B, fluorescence clearing is significantly faster in *Klk5*$^{-/-}$ than in wt mice. Accelerated epidermal proliferation and turnover [19,25] are related to faster wound healing [25]. Therefore to further support our findings, we induced wounds in wt and *Klk5*$^{-/-}$ and examined the rate of wound closure. We found that wounds induced on the back of

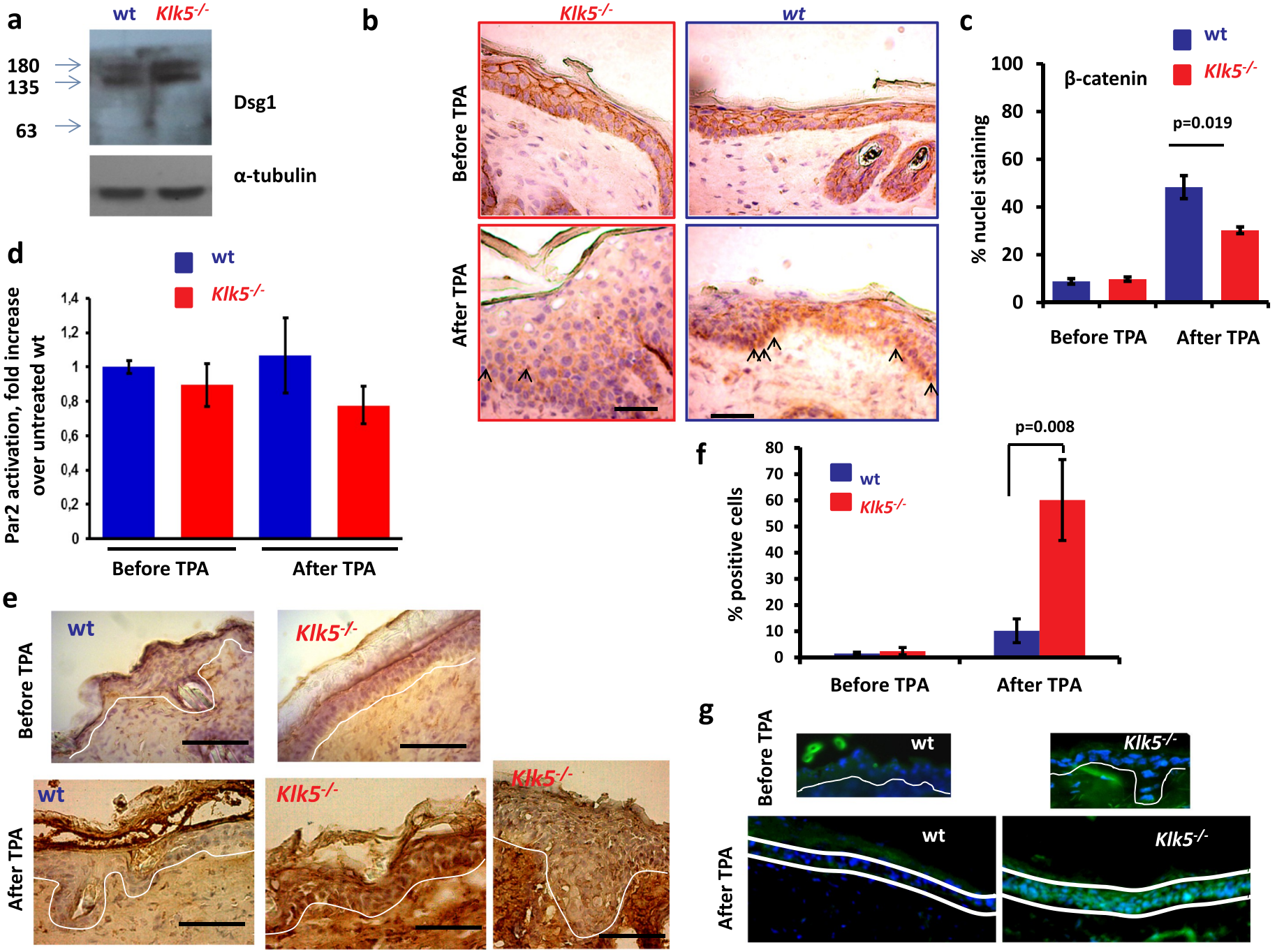

(caption on next page)

Fig. 7. Elimination of Klk5 inhibits β-catenin nuclear localization and induces apoptosis of epidermal cells upon TPA application. **a** After TPA exposure, Dsg1 expression is higher in *Klk5*$^{-/-}$ skin compared to wt. Sizes on the left are given in kDa. **b** IHC analysis of β-catenin expression and localization. After TPA treatment, β-catenin is localized in the nucleus of basal keratinocytes in wt epidermis. Arrows indicate nuclear localization of β-catenin. Not all nuclei have been marked with arrows. Scale bars: 50 μm **c** Quantification of data from b. Data were derived from staining two sections per mouse (n = 3 per genotype) **d** Par2 activation is not altered by TPA. Red bars indicate *Klk5*$^{-/-}$ and blue wt. **e** TPA highly enhances epidermal apoptosis in *Klk5*$^{-/-}$. Apoptosis was tested by the TUNEL assay. Representative images of skin sections from *Klk5*$^{-/-}$ and wt animals. Scale bars: 20 μm. **f** Quantification of data from e. **g** Immunofluorescent (IF) staining for cleaved (*i.e.* active) caspase 3.

Klk5$^{-/-}$ mice tend to heal in a significantly higher rate (Fig. 8C–D). We next focused on understanding how the absence of *Klk5* could affect epidermal proliferation and turnover.

4. Discussion

In the present study we provide a direct link between desmosomes and skin cancer. While it is well-established that desmosomes are essential for skin barrier homeostasis, their putative implication in cancer remains largely unexplored mainly because ablation of main desmosomal proteins results in perinatal lethality [1]. In the opposite, invalidation of *Klk5* elevated the number of desmosomes without inducing any other obvious changes which allowed us to investigate whether altering the number of desmosomes, thereby epidermal microstructure, would affect the development of skin cancer.

We subjected *Klk5*$^{-/-}$ mice to chemical carcinogenesis, an inflammation-driven process [26] and found that they are less susceptible to skin tumor formation than wt mice, suggesting that desmosomes aptly act to suppress tumor formation *in vivo* a hitherto-unknown function. It has been proposed that in skin barrier defect characteristic of NS, hyperactivity of epidermal Klk5 drives inflammation by proteolytic activation of Par2 signaling and/or generation of cathelicidin-derived proinflammatory peptides, while both pathways lead to constitutive activation of the Nf-κb [17,27]. We reasonably expected that elimination of Klk5 would diminish Nf-κb activity and reduce the inflammatory response, which would explain why we observed lower incidence of skin tumors in *Klk5*$^{-/-}$ mice. Unexpectedly, we found higher epidermal Nf-κb activity and increased inflammation in the absence of Klk5.

We show that, in *Klk5*$^{-/-}$ epidermis, β-catenin remains in the cytoplasm upon stimulation with TPA due to the high number of desmosomes, while it is translocated into the nucleus in wt epidermis. It has been demonstrated that increased mechanical stress activates β-catenin pathway in the early stages of colon carcinogenesis [28]. Therefore mechanical resistance would inhibit the induction of tumorigenic β-catenin pathway as we suggest here. Also, we found that the overall proteolytic activities are highly induced in wt but to a much lesser extent in *Klk5*$^{-/-}$ skin. Under conditions of diminished proteolysis, the high levels of Dsg1 are maintained.

Previously it was shown that mice deficient for *Itga3* display epidermal hyperproliferation, accelerated turnover [19,25] and rapid wound healing [25], which are in agreement with our observations. In addition, loss of *Perp* that contributes to desmosomes formation impairs wound healing *in vivo* [35]. The authors suggested that promotion of cellular adhesion is important for wound closure. These data are consistent with our findings since we have stronger adhesion and thus faster wound healing rates. Activation of β-catenin also inhibits the wound healing process [29] and absence of Klk5 prevents its activation that assists in faster wound healing rates.

β-catenin has been reported to promote non-melanoma skin cancer [24] and β-catenin deletion in established DMBA/TPA tumors leads to complete regression [30]. Further, the promoting role of β-catenin activation in cancer is corroborated by the finding of activating mutations in the N-terminal segment of β-catenin in human skin cancers [31]. We

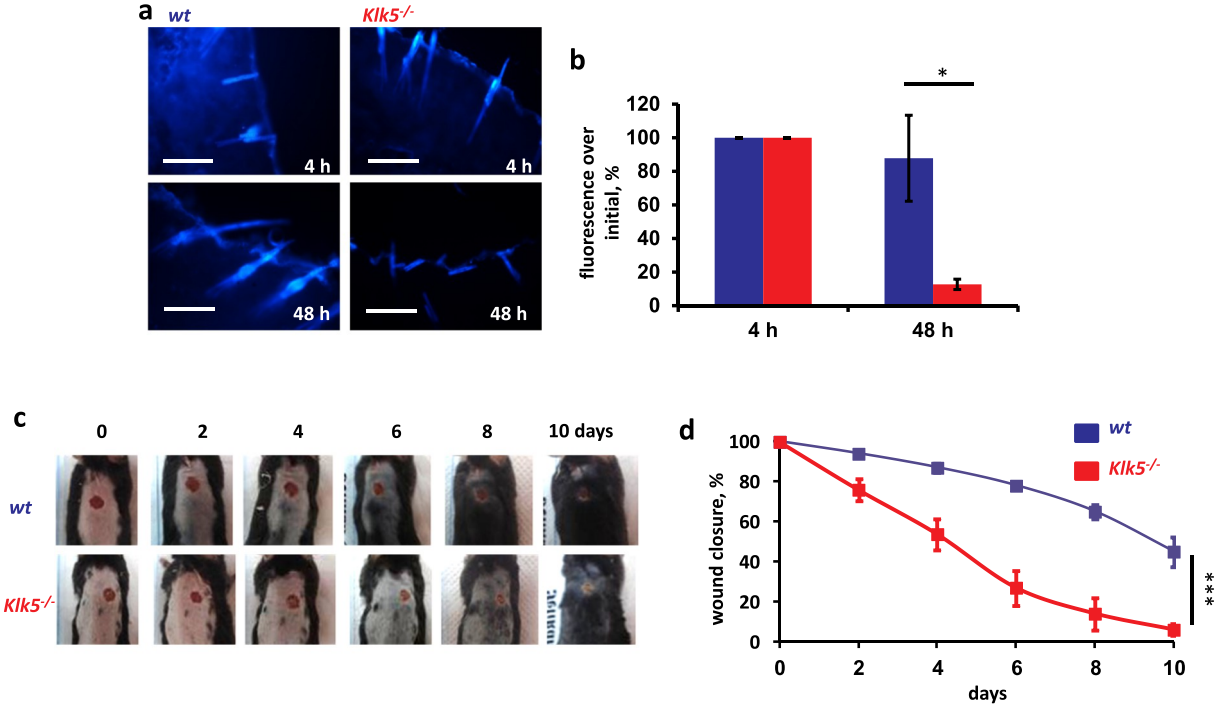

Fig. 8. *Klk5*$^{-/-}$ mice exhibit rapid epidermal turnover and accelerated wound healing. **a** Fluorescence microscopy images of dansyl-labeled skin sections from *Klk5*$^{-/-}$ and wt. **b** Quantification of fluorescence quenching with Image J (n = 4 wt and 3 *Klk5*$^{-/-}$ animals). **c** Representative pictures from the wound healing experiment. **d** Quantification of wound closure. Data were obtained from n = 6 and 3 *Klk5*$^{-/-}$ and wt animals respectively and are shown as mean ± SE. Scale bars: 20 μm. ***p < 0.001.

propose that high number of desmosomes immobilize β-catenin into the cytoplasm, which could explain why skin tumor formation is suppressed in *Klk5*$^{-/-}$. Higher epidermal turnover rates suppress the initiation of skin tumors by depleting the DMBA-mutated keratinocyte stem cells before they acquire further mutations and become malignant [19]. Rapid epidermal turnover in *Klk5*$^{-/-}$ indicates faster epidermal regeneration that is reported to inversely correlate with cancer susceptibility [32,33]. This inverse correlation that was established based on observations in amphibians where it is difficult to induce chemical carcinogenesis and cancer could only be induced in body sites with little capacity to regenerate [32,33]. Here we provide direct *in vivo* evidence that epidermal regeneration is tumor suppressing in mammals.

Previously, it was shown that *in vitro* knockdown of KLK5 expression in oral squamous carcinoma cells prevented DSG1 cleavage, and increased the number of desmosomes [34]. By reinforcing adhesion, repression of KLK5 resulted in reduced dissemination of cancer cells. Contrary, KLK5 overexpression in normal oral keratinocytes resulted in DSG1 cleavage, delayed cell aggregation kinetics and cellular cohesion [34]. However, the actual effect of KLK5 *in vivo* was unknown. Here we showed that Klk5 *in vivo* could facilitate the early stages of tumorigenesis. Indeed analysis of clinical samples from normal skin and various stages of skin cancer revealed absence of KLK5 expression in more advanced stages, pointing to a potential tumor suppressor role at the later stages. It is reasonable to assume that in the later stages the increase of inflammatory reaction that takes place due to the absence of Klk5 may take over to increase the rate of tumor progression.

Cumulatively, we have shown that skin tumor formation is suppressed in Klk5-deficient mice that have a normal epidermal barrier although with increased numbers of desmosomes. We propose that skin desmosomes act as tumor suppressors by inhibiting the translocation of β-catenin into the nucleus. For the first time, the epidermis microstructure is linked to skin tumorigenesis *in vivo*.

Supplementary data to this article can be found online at https://doi.org/10.1016/j.bbadis.2019.07.014.

Transparency document

The Transparency document associated with this article can be found, in online version.

Abbreviations

DMBA	7,12-dimethylbenz[*a*]anthracene
DSG1	desmoglein 1
H&E	haematoxylin-eosin
ICD	irritant contact dermatitis
IF	immunofluorescence
IHC	immunohistochemistry
KLK	human kallikrein-related peptidase
Klk	mouse kallikrein-related peptidase
OCT	optimal cutting temperature
SEM	scanning electron microscopy
TPA	12-O-tetradecanoylphorbol-13-acetate
TEM	transmission electron microscopy
TUNEL	terminal deoxynucleotidyl transferase-mediated dUTP nick end labeling

Acknowledgements

We would like to thank Drs. Timothy S. Blackwell and Fiona E. Yull (Vanderbilt University School of Medicine, Nashville, TN) for kindly providing the *Ngl* mice, Prof. Eleftherios P. Diamandis (Mount Sinai Hospital, Toronto, Ontario, Canada) for the anti-KLK5 antibody, Margarita Chrysanthou-Piterou and Ismini Kloukina (Laboratory of Electron Microscopy, Aeginiteion Hospital, Athens, Greece) and Vassilis Kotsopoulos (Laboratory of Electron Microscopy and Microanalysis, University of Patras, Greece) for technical assistance in TEM and SEM respectively, and Malamati Vreka for data acquisition in *in vivo* imaging experiments.

Declaration of competing interest

The authors declare no competing interests.

Funding

In part, the research project (Skink5 LS4-2139) is implemented within the framework of the Action «Supporting Postdoctoral Researchers» of the Operational Program “Education and Lifelong Learning” (Action's Beneficiary: General Secretariat for Research and Technology), and is co-financed by the European Social Fund (ESF) and the Greek State.

References

[1] R.L. Dusek, L.D. Attardi, Desmosome downregulation is one in a series of steps occurring during cancer development, Nat. Rev. Cancer 11 (2011) 317–323.
[2] M.J. Hardman, K. Liu, A.A. Avilion, A. Merritt, K. Brennan, D.R. Garrod, C. Byrne, Desmosomal cadherin misexpression alters beta-catenin stability and epidermal differentiation, Mol. Cell. Biol. 25 (2005) 969–978.
[3] C.L. Simpson, D.M. Patel, K.J. Green, Deconstructing the skin: cytoarchitectural determinants of epidermal morphogenesis, Nat Rev Mol Cell Biol. 12 (2011) 565–580.
[4] J.R. Stanley, T. Nishikawa, L.A. Diaz, M. Amagai, Pemphigus: is there another half of the story? J Invest Dermatol. 116 (2001) 489–490.
[5] M. Amagai, N. Matsuyoshi, T.H. Wang, C. Andl, J.R. Stanley, Toxin in bullous impetigo and staphylococcal scalded-skin syndrome targets desmoglein 1, Nat. Med. 6 (2000) 1275–1277.
[6] L. Samuelov, O. Sarig, R.M. Harmon, D. Rapaport, A. Ishida-Yamamoto, O. Isakov, J.L. Koetsier, A. Gat, I. Goldberg, R. Bergman, R. Spiegel, O. Eytan, S. Geller, S. Peleg, N. Shomron, C.S. Goh, N.J. Wilson, F.J. Smith, E. Pohler, M.A. Simpson, W.H. McLean, A.D. Irvine, M. Horowitz, J.A. McGrath, K.J. Green, E. Sprecher, Desmoglein deficiency results in severe dermatitis, multiple allergies and metabolic wasting, Nat. Genet. 45 (2013) 1244–1248.
[7] V.G. Beaudry, D. Jiang, R.L. Dusek, E.J. Park, S. Knezevich, K. Ridd, H. Vogel, B.C. Bastian, L.D. Attardi, Loss of the p53/p63 regulated desmosomal protein Perp promotes tumorigenesis, PLoS Genet. 6 (2010) e1001168.
[8] V.G. Beaudry, R.A. Ihrie, S.B. Jacobs, B. Nguyen, N. Pathak, E. Park, L.D. Attardi, Loss of the desmosomal component Perp impairs wound healing in vivo, Dermatol Res Pract. 759731 (2010) 2010b.
[9] M.G. Lawrence, J. Lai, J.A. Clements, Kallikreins on steroids: structure, function, and hormonal regulation of prostate-specific antigen and the extended kallikrein locus, Endocr. Rev. 31 (2010) 407–446.
[10] G. Sotiropoulou, G. Pampalakis, E.P. Diamandis, Functional roles of human kallikrein-related peptidases, J. Biol. Chem. 284 (2009) 32989–32994.
[11] C.A. Borgoño, I.P. Michael, N. Komatsu, A. Jayakumar, R. Kapadia, G.L. Clayman, G. Sotiropoulou, E.P. Diamandis, A potential role for multiple tissue kallikrein serine proteases in epidermal desquamation, J. Biol. Chem. 282 (2007) 3640–3652.
[12] C. Caubet, N. Jonca, M. Brattsand, M. Guerrin, D. Bernard, R. Schmidt, T. Egelrud, M. Simon, G. Serre, Degradation of corneodesmosome proteins by two serine proteases of the kallikrein family, SCTE/KLK5/hK5 and SCCE/KLK7/hK7, J Invest Dermatol. 122 (2004) 1235–1244.
[13] C. Bonnart, C. Deraison, M. Lacroix, Y. Uchida, C. Besson, A. Robin, A. Briot, M. Gonthier, L. Lamant, P. Dubus, B. Monsarrat, A. Hovnanian, Elastase 2 is expressed in human and mouse epidermis and impairs skin barrier function in Netherton syndrome through filaggrin and lipid misprocessing, J. Clin. Invest. 120 (2010) 871–882.
[14] M. Brattsand, K. Stefansson, C. Lundh, Y. Haasum, T. Egelrud, A proteolytic cascade of kallikreins in the stratum corneum, J Invest Dermatol. 124 (2005) 198–203.
[15] C. Deraison, C. Bonnart, F. Lopez, C. Besson, R. Robinson, A. Jayakumar, F. Wagberg, M. Brattsand, J.P. Hackem, G. Leonardsson, A. Hovnanian, LEKTI fragments specifically inhibit KLK5, KLK7, and KLK14 and control desquamation through a pH-dependent interaction, Mol. Biol. Cell 18 (2007) 3607–3619.
[16] M.B. Everhart, W. Han, T.P. Sherrill, M. Arutiunov, V.V. Polosukhin, J.R. Burke, R.T. Sadikot, J.W. Christman, F.E. Yull, T.S. Blackwell, Duration and intensity of NF-kB determine the severity of endotoxin-induced acute lung injury, J. Immunol. 176 (2006) 4995–5005.
[17] A. Briot, C. Deraison, M. Lacroix, C. Bonnart, A. Robin, C. Besson, P. Dubus, A. Hovnanian, Kallikrein 5 induces atopic dermatitis-like lesions through PAR2-mediated thymic stromal lymphopoietin expression in Netherton syndrome, J. Exp. Med. 206 (2009) 1135–1147.
[18] D.A. Quigley, M.D. To, J. Pérez-Losada, F.G. Pelorosso, J.H. Mao, H. Nagase, D.G. Ginzinger, A. Balmain, Genetic architecture of mouse skin inflammation and tumour susceptibility, Nature. 458 (2009) 505–508.
[19] N. Sachs, P. Secades, L. van Hulst, M. Kreft, J.Y. Song, A. Sonnenberg, Loss of

integrin α3 prevents skin tumor formation by promoting epidermal turnover and depletion of slow-cycling cells, Proc. Natl. Acad. Sci. U. S. A. 109 (2012) 21468–21473.
[20] L. Furio, G. Pampalakis, I.P. Michael, A. Nagy, G. Sotiropoulou, A. Honvanian, KLK5 inactivation reverses cutaneous hallmarks of Netherton syndrome, PLoS Genet. 11 (2015) e1005389.
[21] G. Pampalakis, E. Zingkou, G. Sotiropoulou, KLK5, a novel potential suppressor of vaginal carcinogenesis, Biol. Chem. 399 (2018) 1107–1111.
[22] J.J. Johnson, D.L. Miller, R. Jiang, et al., Protease-activated receptor-2 (PAR-2)-mediated Nf-kB activation suppresses inflammation-associated tumor suppressor microRNAs in oral squamous cell carcinoma, J. Biol. Chem. 291 (2016) 6936–6945.
[23] J.K. Nag, T. Rudina, M. Maoz, S. Grisaru-Granovsky, B. Uziely, R. Bar-Shavit, Cancer driver G-protein coupled receptor (GPCR) induced β-catenin nuclear localization: the transcriptional junction, Cancer Metastasis Rev. 2018 (37) (2017) 147–157.
[24] S. Beronja, P. Janki, E. Heller, W.H. Lien, B.E. Keyes, N. Oshimori, E. Fuchs, RNAi screens in mice identify physiological regulators of oncogenic growth, Nature. 501 (2013) 185–190.
[25] C. Margadant, K. Raymond, M. Kreft, N. Sachs, H. Janssen, A. Sonnenberg, Integrin α3β1 inhibits directional migration and wound re-epithelialization in the skin, J. Cell Sci. 122 (2006) 278–288.
[26] E.L. Abel, J.M. Angel, K. Kiguchi, J. DiGiovanni, Multi-stage chemical carcinogenesis in mouse skin: fundamentals and applications, Nat. Protoc. 4 (2009) 1350–1362.
[27] K. Yamasaki, A. Di Nardo, A. Bardan, M. Murakami, T. Ohtake, A. Coda, R.A. Dorschner, C. Bonnart, P. Descargues, A. Hovnanian, V.B. Morhenn, R.L. Gallo, Increased serine protease activity and cathelicidin promotes skin inflammation in rosacea, Nat. Med. 13 (2007) 975–980.
[28] M.E. Fernández-Sánchez, S. Barbier, J. Whitehead, G. Béalle, A. Michel, H. Latorre-Ossa, C. Rey, L. Fouassier, A. Claperon, L. Brullé, E. Girard, N. Servant, T. Rio-Frio, H. Marie, S. Lesieur, C. Housset, J.L. Gennisson, M. Tanter, C. Ménager, S. Fre, S. Robine, E. Farge, Mechanical induction of the tumorigenic β-catenin pathway by tumour growth pressure, Nature. 523 (2015) 92–95.
[29] O. Stojadinovic, H. Brem, C. Vouthouns, B. Lee, J. Fallon, M. Stallcup, A. Merchant, R.D. Galiano, M. Tomic-Canic, Molecular pathogeneis of chronic wounds: the role of beta-catenin and c-myc in the inhibition of epithelialization and wound healing, Am J Pathol. 167 (2005) 59–69.
[30] I. Malanchi, H. Peinado, D. Kassen, T. Hussenet, D. Metzger, P. Chambon, M. Huber, D. Hohl, A. Cano, W. Birchmeier, J. Huelsken, Cutaneous cancer stem cell maintenance is dependent on β-catenin signaling, Nature. 452 (2008) 650–653.
[31] E.F. Chan, U. Gat, J.M. McNiff, E. Fuchs, A common human skin tumour is caused by activating mutations in beta-catenin, Nat. Genet. 21 (1999) 410–413.
[32] J.D. Potter, Morphogens, morphostats, microarchitecture and malignancy, Nat. Rev. Cancer 7 (2007) 464–474.
[33] R.T. Prehn, Regeneration versus neoplastic growth, Carcinogenesis. 18 (2007) 1439–1444.
[34] R. Jiang, Z. Shi, J.J. Johnson, Y. Liu, M.S. Stack, Kallikrein-5 promotes cleavage of desmoglein-1 and loss of cell-cell cohesion in oral squamous cell carcinoma, J. Biol. Chem. 286 (2011) 9127–9135.
[35] V.G. Beaudry, R.A. Ihrie, S.B. Jacobs, B. Nguyen, N. Pathak, E. Park, L.D. Attardi, Loss of the desmosomal component perp impairs wound healing in vivo, Dermatol Res Pract. 2010 (2010) 759731.
[36] R.L. Dusek, S. Getsios, F. Chen, J.K. Park, E.V. Amargo, V.L. Cryns, K.J. Green, The differentiation-depend\ent desmosomal cadherin desmoglein 1 is a novel caspase-3 target that regulates apoptosis in keratinocytes, J Biol Chem. 281 (2006) 3614–3624.
[37] N.K. Veeramachaneni, H. Kubokura, L. Lin, J.A. Pippin, G.A. Patterson, J.A. Drebin, R.J. Battafarano, Down-regulation of beta catenin inhibits the growth of esophageal carcinoma cells, J Thorac Cardiovasc Surg. 127 (2004) 92–98.
[38] L.J. McCawley, J. Wright, B.J. LaFleur, H.C. Crawford, L.M. Matrisian, Keratinocyte expression of MMP3 enhances differentiation and prevents tumor establishment, Am J Pathol. 173 (2008) 1528–1539.